Volcanic activity modulated Holocene extreme hydroclimate events in monsoonal Asia

Weiyi Sun,[1,2,*] Chaochao Gao,[3,*] Xianqiang Meng,[4] and Jian Liu[1,2]

[1]State Key Laboratory of Climate System Prediction and Risk Management/Key Laboratory for Virtual Geographic Environment of Ministry of Education/Jiangsu Center for Collaborative Innovation in Geographical Information Resource Development and Application, Nanjing 210023, China

[2]School of Geography, Nanjing Normal University, Nanjing 210023, China

[3]College of Environmental and Resource Sciences, State Key Laboratory of Soil Pollution Control and Safety, Zhejiang University, Hangzhou 310058, China

[4]State Key Laboratory of Lake Science and Environment, Nanjing Institute of Geography and Limnology, Chinese Academy of Sciences, Nanjing 211135, China

*Correspondence: weiyisun@njnu.edu.cn (W.S.); gaocc@zju.edu.cn (C.G.)

Received: September 16, 2025; Accepted: December 20, 2025; Published Online: December 26, 2025; https://doi.org/10.59717/j.xinn-geo.2026.100187

Citation: Sun W., Gao C., Meng X., et al. (2026). Volcanic activity modulated Holocene extreme hydroclimate events in monsoonal Asia. *The Innovation Geoscience* **4**:100187.

Dear Editor,

Under global warming, extreme hydroclimate events (e.g., droughts and floods) are projected to increase in both frequency and severity, threatening regional economies and ecosystems.[1] However, the short span of observational data limits our understanding of long-term patterns and underlying drivers of such extremes.

The Holocene epoch offers rich geological archives for extending this perspective. Geological records from East and South Asia reveal long-term hydroclimatic variability across the region. For instance, in the middle-lower Yangtze River basin, where the Meiyu front exerts a dominant influence, speleothem magnetic mineral records indicate frequent extreme rainfall events during the early and late Holocene, but relatively quiet period in between (Figure 1A).[2] Similarly, a high-resolution reconstruction from Lake Ximenglongtan—locating at the margin of Indian summer monsoon (ISM)—reveals frequent extreme droughts in the early and late Holocene, with much fewer events during mid-Holocene.[3] Previous studies have often linked these patterns to changes in the El Niño–Southern Oscillation (ENSO) activity, which was weaker during the mid-Holocene and intensified thereafter. However, discrepancies remain between the timing of some extreme hydroclimatic events and reconstructed ENSO activity, suggesting that additional external forcings were influential.

Volcanic eruptions represent a further important forcing that can influence climate extremes.[4] Historical evidence demonstrates that large tropical volcanic eruptions in recent centuries have triggered droughts in the ISM region and flooding in the Yangtze River basin.[5-6] Regrettably, most paleoclimate modeling studies, including the mid-Holocene equilibrium experiments from the Paleoclimate Modelling Intercomparison Project (PMIP3/4) and Holocene transient simulations (e.g., TraCE-21ka), omit volcanic forcing and have generally examined changes in mean-state precipitation rather than extremes. Intriguingly, a recent reconstruction of Holocene volcanic activity reveals high eruption frequencies during the early and late Holocene, with a comparatively quiet interval in the mid-Holocene (Figure 1B).[7] This temporal pattern closely mirrors the prevalence of hydroclimatic extremes, which calls for a systematic examination of their possible connections.

Here we employed the state-of-the-art oxygen isotope-enabled Community Earth System Model version 1.3 (iCESM 1.3) at a horizontal resolution of ~1.9° × 2.5° to conduct a Holocene transient simulation. Crucially, this experiment explicitly incorporates volcanic forcing. Our volcanic forcing is derived from a newly reconstructed eruption sequence based on two high-resolution Holocene ice cores—the Greenland (GISP2) and West Antarctic (WDC) ice cores, which was bias-corrected and verified using 25 Greenland and 38 Antarctic ice cores with representative Common Era volcanic signals. This reconstruction generally aligns with that of Sigl et al.[7] but applies the Gao et al.[8] procedure to prescribe the monthly and spatially dependent forcing index. Additional external forcings include greenhouse gas concentrations, orbital parameters, and ice-sheet changes, similar to recent transient simulation setups.[9] We refer to this experiment as ICE+ORB+GHG+VOL.

To detect extremes in the Holocene climate simulation, we calculate June–August (JJA) precipitation anomalies relative to the 9–1 ka mean. Extreme precipitation in the Yangtze River basin and extreme ISM drought are defined as anomalies above the 98th percentile or falling below the 2nd percentile, respectively, across 9–1 ka. All other values are set to zero. Then, we construct extreme indices by applying a 101-year running mean to highlight their long-term evolution. Moreover, since Holocene volcanic chronology has uncertainties of ±30-50 year, we also apply a 101-year running mean to calculate the accumulative volcanic radiative forcing, which are compared with proxy data.

LINKAGES BETWEEN VOLCANIC ERUPTIONS AND EXTREME HYDROCLIMATIC EVENTS

Visual inspection of the reconstructed volcanic activity with hydroclimatic proxies reveals parallel long-term patterns. During the early Holocene, when eruptions were frequent and intense, hydroclimatic extremes also occurred more often (Figures 1A & B). A notably strong cluster of volcanic eruptions around 8.3, 7.6, and 7.2 ka BP coincided with severe ISM drought and intense Yangtze River flooding. In contrast, during the mid-Holocene interval of reduced volcanism (6.3–3.7 ka BP), such extreme events were far less common. Both volcanism and hydroclimatic extremes intensified again in the late Holocene. The significant correlation ($r = 0.3$, $p < 0.05$, based on the effective degrees of freedom) between the 101-year running mean of volcanic forcing and reconstructed droughts over 9–1 ka BP suggests that volcanic eruptions may have influenced ISM drought occurrence. A weaker but still notable relationship appears in the Yangtze River basin during 8.6–4 ka BP ($r = 0.23$, $p < 0.10$), likely moderated by the growing role of ENSO variability during the mid-to-late Holocene. The consistent correlations between volcanic eruptions and the reconstructed extreme dry–wet indices across the −25 to +25 years lead–lag sensitivity test indicate that dating uncertainties in the records are unlikely to substantially influence our conclusions.

Our modeling results also demonstrate strong coherence between volcanic activity and hydroclimatic extremes (Figure 1C). The 101-year running mean of accumulated volcanic radiative forcing correlates significantly with the ISM drought index ($r = 0.51$, $p < 0.01$) over 9–1 ka, explaining about 25% of the variance. Particularly, the correlation coefficient reaches $r = 0.72$ ($p < 0.01$) during the early Holocene (9–6.5 ka), explaining ~50% of the variance. This is much stronger than during the mid-late Holocene ($r = 0.30$, $p < 0.05$, 6.5–1.0 ka). In the Yangtze River basin, volcanism and floods correlate at $r = 0.31$ ($p < 0.05$) for the overall Holocene (9–1 ka), higher than during the relatively quiet volcanic period ($r = 0.17$, $p > 0.10$, 6.3–3.7 ka). Additionally, we tested different running-mean windows (i.e., 31 to 201 years) and found that all correlations between volcanic forcing and both regional indices remain robust and statistically significant.

To isolate the volcanic signal during the mid-to-late Holocene, when ENSO variability began to intensify, we used a parallel non-volcanic run from the iTraCE. In this run, greenhouse gas, orbital, and ice-sheet forcings are identical to those in our experiment (ICE+ORB+GHG+VOL) over 6.5-0 ka (see Bao et al.[9] for experimental design). Subtracting this background noVOL signal reveals that volcanic eruptions significantly enhance late-Holocene (4–1 ka) ISM droughts, with a correlation of $r = 0.32$ ($p < 0.05$) between volcanic activity and droughts, explaining ~10% of their variance (Figure not shown). Volcanism also contributed moderately to Yangtze River flooding occurrence

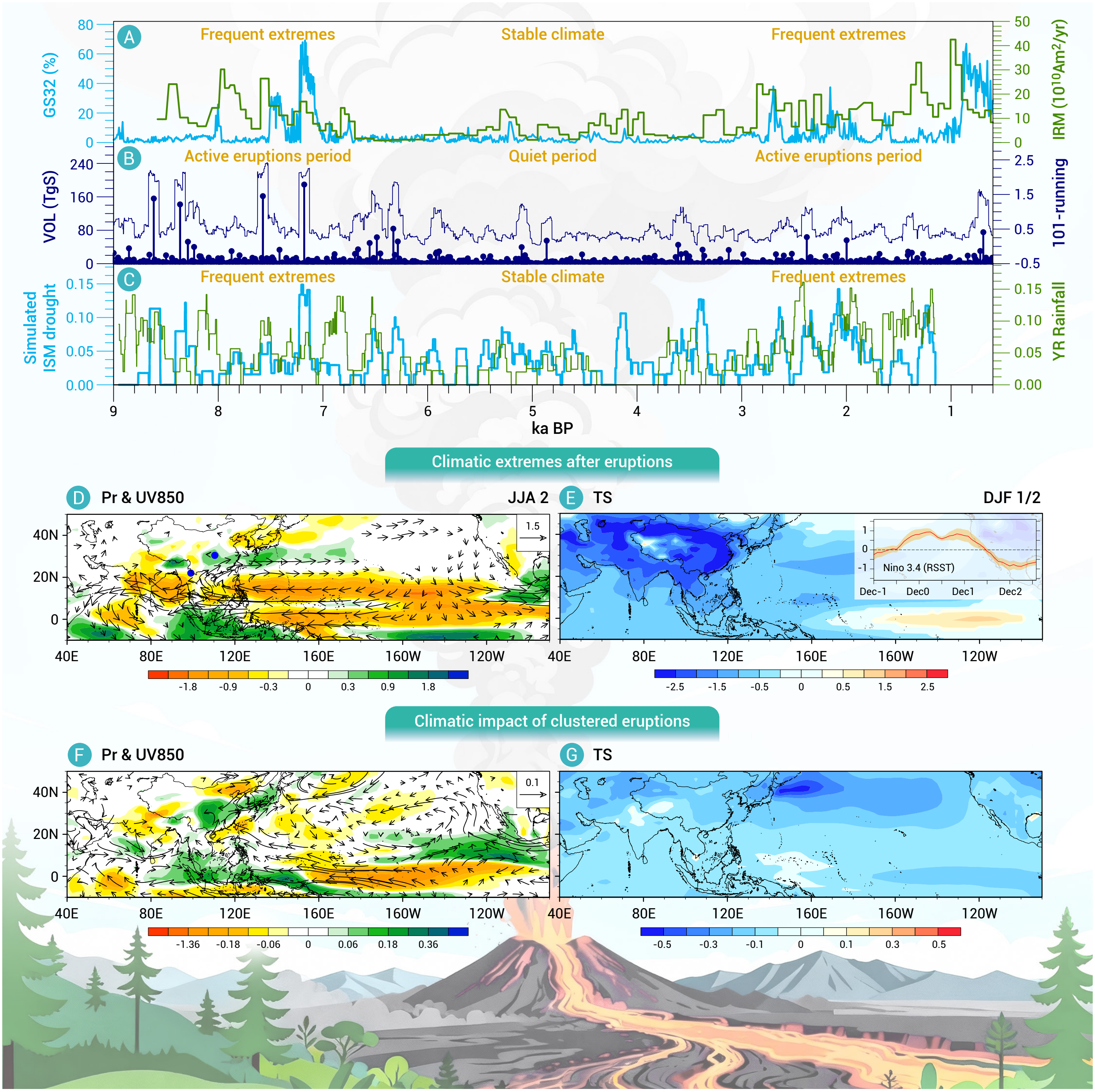

Figure 1. Holocene extreme hydroclimatic events in the ISM region and the Yangtze River basin, and volcanic impact (A) Reconstructed lake level changes (GS32; blue) from Lake Ximenglongtan (22°38′N, 99°35′E)[3] and speleothem magnetic mineral records ($IRM_{soft-flux;}$ green) from Heshang Cave (30°27′N, 110°25′E)[2]. (B) Reconstructed volcanic stratospheric sulfur injection (Tg S)[7] of individual eruption and the perspective 101-year running mean. (C) Simulated extreme droughts in the ISM region (8°–20°N, 70°-100°E; blue) and extreme precipitation in the Yangtze River basin (25°-34°N, 105°-115°E; green). Hydroclimatic extremes are defined by JJA precipitation exceeding the top 2% threshold during 9–1 ka. After constructing the extreme indices, a 101-year running mean is applied. (D) Superposed epoch analysis (SEA) of unsmoothed precipitation (shadings; mm day^{-1}) and 850 hPa winds (vectors; m s^{-1}) anomalies in JJA2 after the top 30 largest eruptions during 9–1 ka. Blue dots denote the locations of two reconstructions. (E) is same as (D), but for surface air temperature anomalies (°C) in the second winter. Time series of anomalous monthly relative SST (RSST, °C) over the Niño-3.4 region after the top 30 largest eruptions are shown in (E), and shadings represent twice the standard error of the mean. The RSST removes the mean tropical (20°S–20°N) SST anomaly and better captures ENSO-related gradients under global cooling.[4] (F) Composite analysis of JJA precipitation and 850 hPa winds anomalies between the clustered large eruptions periods (8.55–8.30, 7.20–7.05, and 6.6–6.3 ka) and the quiet period (6.3–3.7 ka). The data were linearly detrended over 9–1 ka and smoothed with a 101-year running mean before analysis. (G) is same as (F), but for surface air temperature anomalies. In (D-G), only the significant results with confidence levels exceeding 90% (two-tailed Student's t-test) are displayed.

($r = 0.27$, $p < 0.10$), explaining ~7% of the variance, which indicates a weaker sensitivity than in the ISM region.

Overall, both model and reconstructions consistently demonstrate that volcanic forcing strongly influenced ISM droughts and, to a lesser degree, Yangtze floods. It should be noted that some degree of mismatch exists between volcanic eruptions and extreme dry-wet reconstructions, particularly during late Holocene (4-1 ka). This discrepancy may partly arise from the orbital forcing-enhanced ENSO variability during this period, which provided an additional and compounding influence on hydroclimatic extremes during this period.

PHYSICAL PROCESSES LINKING HOLOCENE VOLCANISM WITH HYDROCLIMATE EXTREMES

Volcanic eruption injects aerosols into the stratosphere, reflecting shortwave radiation and cooling surface.[4-6] Holocene records document numerous large volcanic eruptions, with some eruptions far exceeded the magnitude of the well-known 1815 CE Tambora eruption. We select the 30 largest eruptions from our Holocene simulation, with an average size of about 1.3 times the Tambora eruption (37 Tg S), and perform a superposed epoch analysis (SEA) of unsmoothed data. Results indicate that extreme drought occurred across the ISM region in the first boreal summer post-eruption, particularly in India, the southern Tibetan Plateau, the Bay of Bengal, and Southeast Asia (Figure not shown). This response stems from stronger volcanic cooling over the Eurasian and African continents than over tropical oceans, which reduces temperature gradients and weakens the ISM circulation, especially the low-level cross-equatorial Somali Jet. In the second boreal summer, atmospheric aerosol concentrations decline and the cooling effect weakens. A distinct hydroclimatic dipole emerges: precipitation increased significantly in the Yangtze River basin, while drought persists in the ISM region (Figure 1D). This interannual-scale dipole pattern has also been independently confirmed by observations, proxy reconstructions, and other climate model simulations.[5,6,10]

The enhanced Yangtze rainfall is primarily linked to stronger moisture transport by a strengthened western North Pacific anomalous anticyclone (WNPAC),[10] whose development is caused by the rapid transition from the volcano-induced El Niño (+0.76°C) to a La Niña-like state (−0.80°C, Figure 1E).[6] Volcanically induced land–ocean thermal contrasts between Eurasia and the Pacific may influence El Niño development in the first year, after which volcanic forcing amplifies the ENSO transition via the wind–evaporation–SST feedback. Combined with cooler SSTs in the western North Pacific, this feedback extends and intensifies the WNPAC.[6,10]

Clustered large volcanic eruptions can affect decadal-to-centennial climate variability, which may also influence the climatic extremes. To assess this, we composite boreal summer precipitation and atmospheric circulation anomalies during three periods of clustered eruptions (8.55–8.30, 7.20–7.05, and 6.6–6.3 ka) and contrast them with the volcanic-quiet period (6.3–3.7 ka). The accumulative effect of cluster eruptions produces centennial-scale cooling over the Northern Hemisphere (Figures 1F-G) and weakened monsoon circulation over the Indian Continent. The land–sea thermal contrast under successive volcanic eruptions is weaker on decadal-to-centennial timescales than on the interannual scale, resulting in a distinct circulation response. In the tropical Pacific, a prevailing La Niña–like state strengthens the western Pacific subtropical high, enhancing southwesterly winds over southern China. Simultaneously, a weakened meridional temperature gradient limits moisture transport to northern China, concentrating persistent rainfall over the Yangtze River Basin. Moreover, this dipole pattern of ISM drought and Yangtze River flood is reproduced consistently across all three clustered eruption periods. Together, these changes reduce precipitation in the ISM region while increasing precipitation in the Yangtze River basin, promoting hydroclimatic extremes in both regions (Figure 1F).

In summary, we provide first evidence of volcanic eruptions served as a previously underappreciated trigger of Holocene hydroclimatic extremes, which moves beyond the conventional notions linking these extreme events to ENSO variability. By combining a Holocene transient simulation that explicitly incorporates volcanic forcing with reconstructions, we demonstrate that frequent large volcanic eruptions during the early Holocene promoted a recurrent dipole pattern, characterized by severe ISM droughts and intense Yangtze River flooding. These droughts arose from weakened cross-equatorial flow, while flooding was associated with a rapid ENSO transition and a westward strengthened WNPAC. Clusters of large eruptions further induced centennial-scale Northern Hemisphere cooling, which favored the occurrences of extremes. Hydroclimatic extremes in the late Holocene were influenced by both volcanic forcing and orbital forcing-enhanced ENSO variability. However, precisely quantifying the relative contributions of volcanic forcing, internal variability, and other external drivers remains a challenge. Future studies need to conduct ensemble model simulations and higher-resolution or downscaled modeling approaches to better resolve regional extreme events. Furthermore, our findings indicate that future large volcanic eruptions, particularly if clustered, could substantially increase the risk of concurrent ISM droughts and Yangtze River floods. Improving representation of volcanic forcing in climate models is essential for advancing decadal predictions and risk assessments of such compound extremes.

REFERENCES

1. Chen Z., Li X., Zhang X., et al. (2025). Global drought-flood abrupt alternation: Spatiotemporal patterns, drivers, and projections. *Innov. Geosci.* **3**:100113. DOI:10.59717/j.xinn-geo.2024.100113
2. Zhu Z., Feinberg J.M., Xie S., et al. (2017). Holocene ENSO-related cyclic storms recorded by magnetic minerals in speleothems of central China. *Proc. Natl. Acad. Sci. USA* **114**:852–857. DOI:10.1073/pnas.1610930114
3. Zhang E., Meng X., Ning D., et al. (2023). Holocene extreme hydroclimate events in the Asian monsoon region were more frequent during cooler intervals. *Commun. Earth Environ.* **4**:344. DOI:10.1038/s43247-023-00997-x
4. Dogar M.M., Fujiwara M., Zhao M., et al. (2024). ENSO and NAO linkage to strong volcanism and associated post-volcanic high-latitude winter warming. *Geophys. Res. Lett.* **51**:e2023GL106114. DOI:10.1029/2023GL106114
5. Xing C., and Liu F. (2023). Mount Pinatubo eruption caused the major East China flood in 1991. *Innov. Geosci.* **1**:100032. DOI:10.59717/j.xinn-geo.2023.100032
6. Sun W., Chen D., Lü G., et al. (2024). Impacts of major volcanic eruptions over the past two millennia on both global and Chinese climates: A review. *Sci. China Earth Sci.* **67**:61–78. DOI:10.1007/s11430-022-1218-0
7. Sigl M., Toohey M., McConnell J.R., et al. (2022). Volcanic stratospheric sulfur injections and aerosol optical depth during the Holocene (past 11 500 years) from a bipolar ice-core array. *Earth Syst. Sci. Data* **14**:3167–3196. DOI:10.5194/essd-14-3167-2022
8. Gao C., Robock A., and Ammann C. (2008). Volcanic forcing of climate over the past 1500 years: An improved ice core-based index for climate models. *J. Geophys. Res.* **113**:D23. DOI:10.1029/2008JD010239
9. Bao Y., Liu Z., Thompson L.G., et al. (2025). Climate simulations and ice core data highlight the Holocene conundrum over tropical mountains. *Commun. Earth Environ.* **6**:205. DOI:10.1038/s43247-025-02188-2
10. Liu F., Gao C., Chai J., et al. (2022). Tropical volcanism enhanced the East Asian summer monsoon during the last millennium. *Nat. Commun.* **13**:3429. DOI:10.1038/s41467-022-31108-7

FUNDING AND ACKNOWLEDGMENTS

This work was supported by the National Natural Science Foundation of China (42130604), the National Key Research and Development Program of China (2023YFF0804704), and A Project Funded by the Priority Academic Program Development of Jiangsu Higher Education Institutions (164320H116). The funders had no role in study design, data collection and analysis, decision to publish, or preparation of the manuscript.

AUTHOR CONTRIBUTIONS

All authors contributed to the manuscript and approved the final version.

DECLARATION OF INTERESTS

The authors declare no competing interests.